Exp Astron (2014) 37:579–598
DOI 10.1007/s10686-014-9389-y

ORIGINAL ARTICLE

THz photometers for solar flare observations from space

Pierre Kaufmann · Rogério Marcon · André Abrantes · Emilio C. Bortolucci · Luis Olavo T. Fernandes · Grigory I. Kropotov · Amauri S. Kudaka · Nelson Machado · Adolfo Marun · Valery Nikolaev · Alexandre Silva · Claudemir S. da Silva · Alexander Timofeevsky

Received: 19 February 2014 / Accepted: 22 April 2014 / Published online: 21 May 2014

Abstract The search for the still unrevealed spectral shape of the mysterious THz solar flare emissions is one of the current most challenging research issues. The concept, fabrication and performance of a double THz photometer system, named SOLAR-T, is presented. Its innovative optical setup allows observations of the full solar disk and the detection of small burst transients at the same time. The detecting

P. Kaufmann (✉) · L. O. T. Fernandes · A. S. Kudaka
Escola de Engenharia, CRAAM, Universidade Presbiteriana Mackenzie, São Paulo, SP, Brazil
e-mail: pierrekau@gmail.com

P. Kaufmann · E. C. Bortolucci
Centro de Componentes Semicondutores, Universidade Estadual de Campinas, Campinas, SP, Brazil

R. Marcon
Instituto de Física Gleb Wataghin, Universidade Estadual de Campinas, Campinas, SP, Brazil

R. Marcon
Observatório Solar "Bernard Lyot", Campinas, SP, Brazil

A. Abrantes · N. Machado
Propertech Ltda., Jacareí, SP, Brazil

A. Marun
Complejo Astronômico El Leoncito, CONICET, San Juan, Argentina

A. Silva
Samsung Research Institute, Campinas, SP, Brazil

C. S. da Silva
Neuron Ltda., São José dos Campos, SP, Brazil

G. I. Kropotov · V. Nikolaev · A. Timofeevsky
Tydex, LLC, Saint Petersburg, Russia

system was constructed to observe solar flare THz emissions on board of stratospheric balloons. The system has been integrated to data acquisition and telemetry modules for this application. SOLAR-T uses two Golay cell detectors preceded by low-pass filters made of rough surface primary mirrors and membranes, 3 and 7 THz band-pass filters, and choppers. Its photometers can detect small solar bursts (tens of solar flux units) with sub second time resolution. Tests have been conducted to confirm the entire system performance, on ambient and low pressure and temperature conditions. An artificial Sun setup was developed to simulate performance on actual observations. The experiment is planned to be on board of two long-duration stratospheric balloon flights over Antarctica and Russia in 2014–2016.

Keywords THz photometers · Solar flares · Stratospheric balloon platform · THz detectors · THz photometer performance · Solar flare THz emissions

1 Introduction

A number of solar bursts observed at sub-THz and 30 THz frequencies indicate an emission spectral component at this range [1–3], distinct from the well known microwave emission that maximizes at few to tens GHz. These results raise serious interpretation problems to explain both the sub-THz and the concurrent microwave component [4, 5]. The physical nature of the THz emission remains mysterious. New insights on the physical processes involved require the complete THz spectral description. This can be accomplished by observations with detectors placed outside the terrestrial atmosphere, as it has been done at far IR for non-solar experiments on SOFIA high altitude aircraft [6], PACS experiment on HERSCHEL satellite [7] and solar scanning experiment on a stratospheric balloon [8]. Experiments SIRE [9] and DESIR [10] to observe solar flares in the THz range from space have been proposed. Solar activity can also be observed through a few atmospheric THz transmission "windows" at exceptionally good high altitude ground based locations [11, 12].

The practical problem to observe the whole solar disk with enough sensitivity to detect flares subtended by much smaller angular sizes was solved with an innovative photon concentrator [13, 14] that combines the formation of a full solar disk image at the focal plane with size smaller than the size of the surface of the detecting element (or of the photon concentrator aperture), with the physical size of telescope primary aperture, as described below. It becomes possible to use apertures large enough to detect small solar bursts without the need to point at a particular location on the solar disk with narrow beams, as in usual coherent optical configurations.

The THz solar photometer system, named SOLAR-T, is the result of nearly ten years of research, detecting devices development and characterization of materials, filters and systems. Several prototypes have been built and tested for their performances [15–17]. Here we describe the definitive flight system that has been built, integrated to data acquisition and telemetry modules developed for this application, and tested in Brazil. It utilizes two of a modern version of Golay cell detectors ([18],

http://www.tydexoptics.com/pdf/Golay_cell.pdf) preceded by low-pass filters made of rough surface primary mirrors [19, 20] and membranes (http://www.tydexoptics.com/pdf/THz_Materials.pdf (2014)) to suppress visible and near IR radiation, 3 and 7 THz metal mesh band-pass filters [21, 22], and choppers. The SOLAR-T photometers can detect excess temperature variations smaller than 0.5 K with sub second time resolution, which corresponds to bursts of moderate intensity (1–2 hundred SFU, 1 SFU $= 10^{-22}$ W m^{-2} Hz^{-1}).

2 The high gain full solar disk photon concentrator concept

Two known independent telescope properties were combined in order to obtain a sufficiently large gain to detect small bursts that may pop up at any place on the solar disk, while observing the whole field containing the solar disc [13, 14]. Figure 1 illustrates the ray tracings for solar disk image formed, with size d, at the focal plane of a reflector aperture with diameter D. The same geometry is applicable for a lens aperture. The solar disk angular dimension is θ. The solar disk image size d relates to the aperture's focal length as $f = d/tan\ \theta$, which is independent from the aperture diameter and from wavelength. On the other hand the aperture's gain is directly proportional to its surface, $G = 4\pi A_e/\lambda^2$, where λ is the wavelength, the effective area $A_e = \eta A$, where η is the net aperture efficiency and the physical area

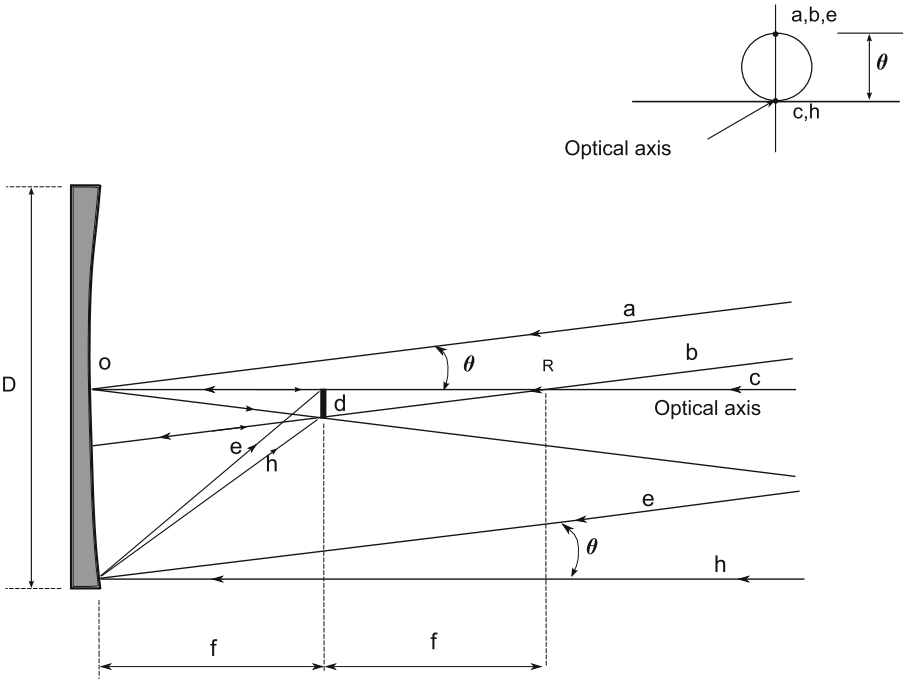

Fig. 1 The principle of image formation with size d for a distant source with angular size θ at the focal plane of an aperture, set by d = f tan θ, which is independent from the aperture diameter D and wavelength λ. The sensitivity to detect excess radiation can be enhanced for larger diameters

$A = \pi(D/2)^2$ (see [23], and references therein). Therefore it becomes possible to enlarge the diameter D to obtain sufficiently large gain needed to detect a certain level of flux, keeping the same focal length. For aperture diameters above a certain size, enhanced aberrations shall produce a blurred disc image. This is not a problem for photometry purposes because all disc and burst photons are detected. The radiation by burst excess is added to the whole solar disk background, concentrated on the detecting device surface.

A schematic illustration of a solar disk scan is shown in Fig. 2. The output voltage is proportional to the input power, or equivalent flux density. It corresponds to the solar disk image d displacing over the detecting area, which may be represented by a photon collecting cone aperture with diameter L. The corresponding angular displacements correspond to the solar image size d displacement to fill the collecting aperture of size $L(\theta_A)$. The displacement between the extremes (θ_B) is sometimes called "acceptance angle". This was reproduced in laboratory and it is shown in Section 5.

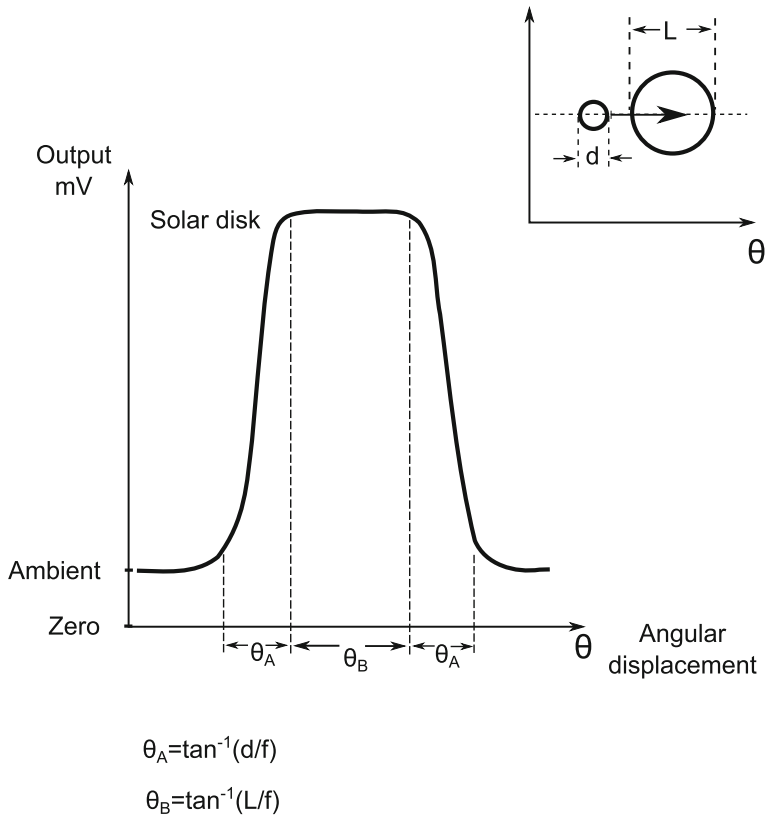

Fig. 2 The solar disk scan in units of angular displacement. It corresponds to the solar disk solar image size d, displacement over the detecting device aperture L (*upper drawing*) at the focal plane. The system output is in voltages proportional to power

3 The THz photometers construction

Figure 3 illustrates the SOLAR-T design conception. The final system has been derived from several characterizations and tests of materials, filters, sensors and the performance of actual complete operational prototypes [14–17]. The two 76 mm diameter Cassegrain telescopes have focal length of 580 mm. For the Sun angular diameter of 0.5° they produce a 5 mm solar image, smaller than the Golay cell input cone aperture (10 mm) (http://www.tydexoptics.com/pdf/Golay_cell.pdf). The Cassegrain primary reflector has been roughened [19, 20] to diffuse part of the visible and near IR, delivering a "cool" solar signal into the detecting system, consisting of TPX windows, resonant fork chopper, metal mesh band-pass filter and the Golay cell, as described below. The resonant fork chopper (http://www.eopc.com/ch10_ch20.html (2012)) has been selected for its small size and negligible mechanical coupling to the Golay cell.

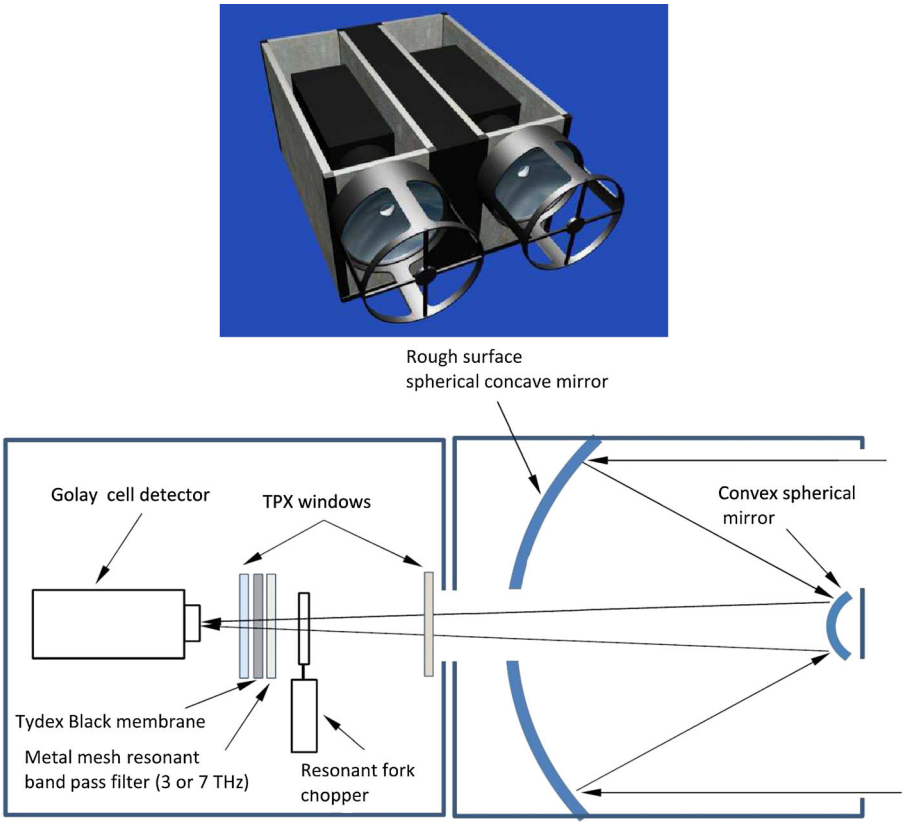

Fig. 3 The SOLAR-T photometer assembly concept. The diagram in the *bottom panel* shows on the left the Golay cell detector, preceded by TydexBlack low-pass filter membrane, a resonant metal mesh band-pass filter, and a resonant tuning fork 20 Hz chopper. The 76 mm Cassegrain telescope on the right has a rough surface to further diffuse the visible and near IR radiation. TPX windows were added to separate the telescopes from the case

3.1 Low-pass and band-pass filters

Most of the solar disk radiation power is in the visible and near IR range which must be suppressed not only to protect the detecting devices, but mainly to assure that no parasite high frequency radiation component enters into the sensing system. The diffusion of visible and near IR by reflection in rough surfaces has been proposed for another space experiment [9, 19] and tested for flat mirrors with different grains used in roughening [20]. The primary 76 mm concave Cassegrain reflectors of SOLAR-T have been grinded at "Bernard Lyot" Solar Observatory facilities using Caborundum 10 μm particles, which produced a roughening of about 1.25 μm r.m.s. [20]. The reflection losses at THz have been measured at CCS/Unicamp, using one Golay cell detecting system setup, similar to the concept shown in Fig. 3, and a heated blackbody source large enough to cover entirely the telescope aperture (one heating muffle). Two Cassegrain telescopes identical to the SOLAR-T units (Fig. 4) have been built separately: one aperture with perfect optically polished surface and another with rough surface, both aluminized. Using metal mesh band-pass filter at 2 THz, the power transmission for the rough mirror was reduced by 10 % compared to the optical polished mirror. The transmission was assumed to be similar for the two SOLAR-T frequencies.

The 3 and 7 THz band-pass filters were produced using the metal mesh resonant model predictions and fabrication techniques described in [21, 22]. The measured transmission shown in Fig. 5 is from the sandwich made of the BlackTydex membrane, TPX (http://www.tydexoptics.com/pdf/THz_Low_Pass_Filter.pdf (2012)), and the band-pass filters have been optimized and measured at Tydex, before being installed within the box containing the SOLAR-T. We have obtained a total net transmission performance close to the predictions: of about 35 % at 3 THz and 29 % at 7 THz, and band-pass of 16.7 % and 13.7 % of the central frequencies, respectively [15, 22].

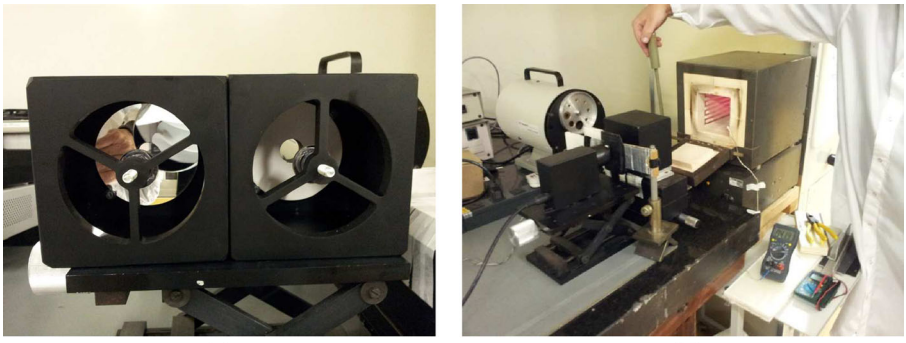

Fig. 4 **a** Two telescopes identical to those used in SOLAR-T were built to measure the losses of a rough surface compared to a polished mirror. **b** A furnace radiator on the right, large enough to cover the whole telescope aperture was heated at a fixed high temperature. The output using the polished and the roughened telescopes were made alternatively, using a 2 THz band-pass filter. The transmission by the rough surface mirror was about 0.9 compared to the polished mirror

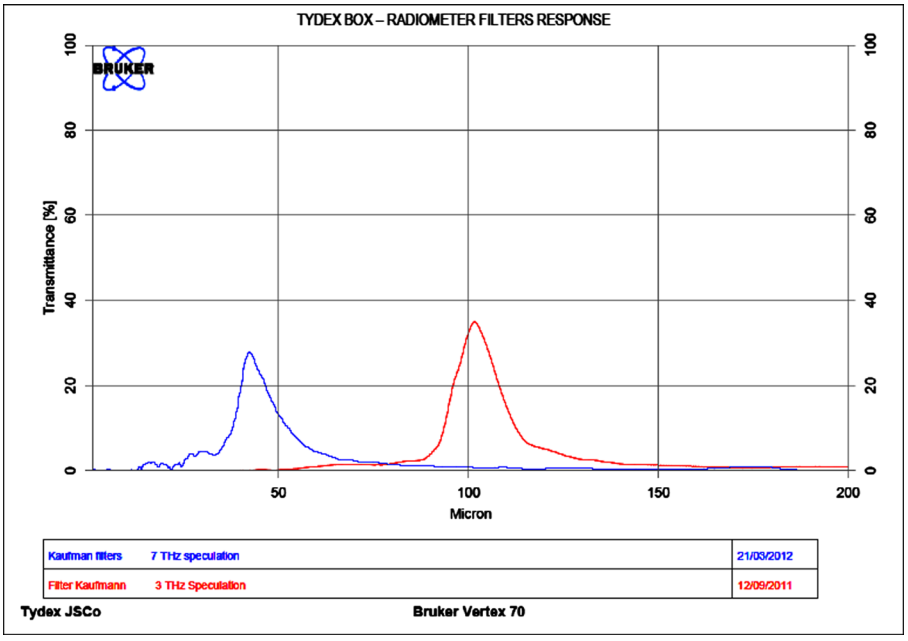

Fig. 5 The optimized total transmission of the combined TPX windows, TydexBlack low pass filter membrane and band-pass resonant metal mesh filters centred at 3 and 7 THz

3.2 The 3 and 7 THz photometers construction

The double THz photometers SOLAR-T system was built by Tydex LLC., St. Petersburg, Russia, where they were tested for electrical, electronics, low temperature and near vacuum environment performance. The data acquisition system was developed by Propertech Ltda., Jacareí, SP, Brazil, which, also, has integrated the whole system, to which was included an Iridium-satellite telemetry module, provided by Neuron Ltda., São José dos Campos, SP, Brazil [24]. Figure 6 shows the complete SOLAR-T hardware, in (a), being submitted to the low pressure expected in the stratosphere (1000 Pa, or 7.5 mm Hg) and −25 °C active tests at Tydex LLC in (b), and integrated to the data acquisition and telemetry modules at Propertech in (c). As stated earlier, the 76 mm diameter Cassegrain telescopes have 580 mm focal length to form a 5 mm solar disc image at the 10 mm input cone of the Golay cell (http://www.tydexoptics.com/pdf/Golay_cell.pdf).

The Golay cell sensor [18] consists in a room temperature opto-acoustic detector based on a Xenon gas capsule with a light reflecting flexible membrane surface. With radiation incidence, the gas tends to expand the membrane which deflects the internal light ray into an array of photo-detectors. The device is highly sensitive to small input power variations. Although originally intended for infra-red detection [18], it has shown a nearly flat response from mm- to THz to visible radiation. Modern Golay cell (http://www.tydexoptics.com/pdf/Golay_cell.pdf) exhibits the best

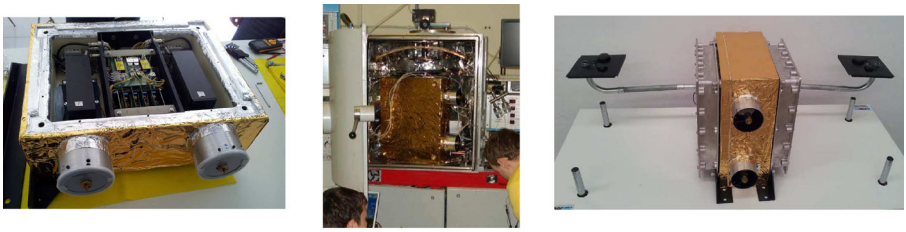

(a) **(b)** **(c)**

Fig. 6 **a** The SOLAR-T case with the 3 and 7 THz photometers, containing the two Golay cells detectors, filters, choppers, ambient temperature devices and electronics. **b** SOLAR-T with active electronics being submitted to low temperatures (−25°) and near vacuum (1000 Pa) at Tydex. **c** The complete experiment integrated to the data acquisition, handling and telemetry modules at Propertech

sensitivity for input signal power variations at THz frequencies compared to other options tested for room temperature detectors: micro-bolometer and pyro-electric [15–17].

3.3 Integration, data acquisition and telemetry

The SOLAR-T was integrated to the data acquisition and telemetry modules developed and fabricated in Brazil by Propertech and Neuron companies, respectively. The block diagram in Fig. 7 shows both modules.

They operate independently, with their own GPS clocks. Each module consists of a CPU that reads output signals from the Golay cell, with an arrangement

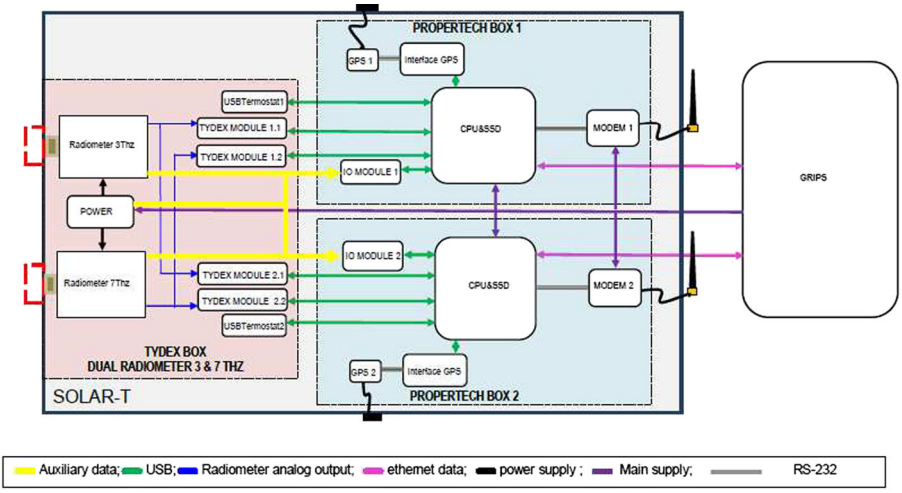

Fig. 7 Block diagram of the data acquisition and telemetry systems

of two data reading modules, to assure redundancy, in the case one of them fails. The input resonant fork choppers operate at 20 Hz close to the optimal Golay cell performance (http://www.tydexoptics.com/pdf/Golay_cell.pdf). The two Golay cells outputs are read by data processing specially developed modules with built-in electronics and software (http://www.tydexoptics.com/products/thz_optics/golaycell_soft/ (2012)) that samples data at a 500 Hz rate (i.e., 0.002 s). The data acquisition allows readings at various selectable modes and gains; by specific software developed for this experiment, named ProSolarT. For the current operational test application, we have adopted successive fast Fourier transforms of 128 output data points sampled every 2 ms, (i.e., 0.256 s time resolution). The readings are stored in the data acquisition module, together with clock reference and auxiliary readings describing the payload status (voltages, temperatures, etc.). Other box parameters, such as temperatures and voltages, are read at slower rates.

Compressed THz photometers data, clock and auxiliary data are interfaced to the telemetry system, based on Iridium satellite network, and are also duplicated for redundancy. The block diagram for the telemetry subsystem is shown in Fig. 8. It is composed by a 9602 Iridium modem (http://www.satrunner.com/en/iridium-9602-sbd-modem.html) and electronic circuitry whose main components are a microcontroller, memory chip, linear regulator and a DC/DC converter. The modem transmits and receives digital data packages through the Iridium SBD—Short Burst Data—service (http://www.wcclp.com/SBD.asp). Data packages transmitted to ground have the maximum size of 340 bytes and those received from ground of 270 bytes. The Iridium satellite network is the best suited for communications in Antarctica where SOLAR-T is planned to be initially flown together with the GRIPS experiment [25].

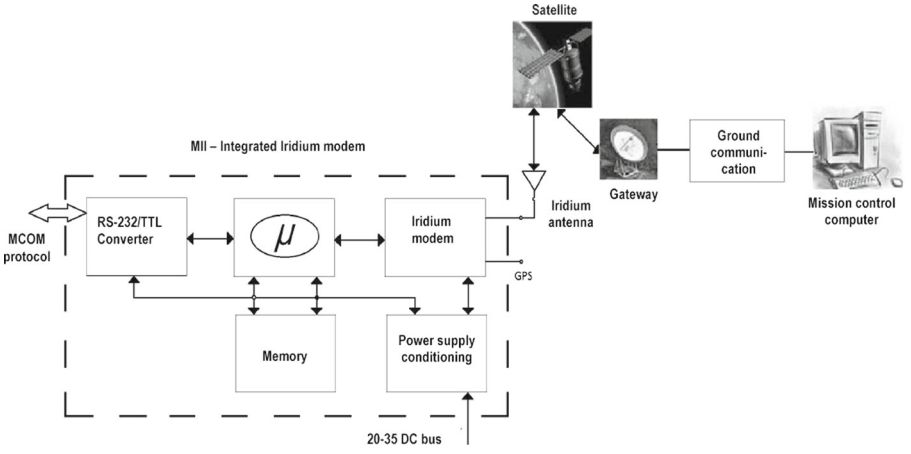

Fig. 8 The Iridium Short Data Burst communication module block diagram for SOLAR-T

4 Tests and performance

4.1 The temperature/output voltage characteristics

The Golay cells have two characteristic response properties which are relevant for the observations proposed here: (1) the noise fluctuation level is constant and the same for the whole range of input temperatures and (2) the voltage outputs are proportional to the input temperatures. The calibration curves shown in Fig. 9 were obtained using a large size blackbody furnace (a heating muffle) to cover the whole telescope aperture, the same shown in Fig. 4b. The temperature vs. voltage plots are characteristic for each photometer and provide conversion factors for temperature variations of 4.2 K/mV at 3 THz and 9.8 K/mV at 7 THz. The result is qualitatively consistent, as expected for two distinct Golay cells, recalling that at 3 THz the blackbody power is smaller than at 7 THz and the frequency band-pass is considerably smaller at 3 THz than at 7 THz (i.e. about 0.4 THz at 3 THz and 1.2 THz at 7 THz, respectively).

4.2 Data acquisition, processing and telemetry

Using the ProSolarT software developed for SOLAR-T THz photometers we show in Fig. 10 how data are acquired, using as an example the 3 THz response to a hot source at an arbitrary temperature placed in front of the telescope. The input is alternatively changed from hot to ambient temperature levels by a resonant fork chopper at a 20 Hz rate. In Fig. 10a there is a sample of the five cycles of the output waveform taken at a 500 Hz rate (2 ms), showing the response to the 20 Hz input chopper. Figure 10b shows the Fourier transform for 128 data points (i.e. taken every 256 ms) which

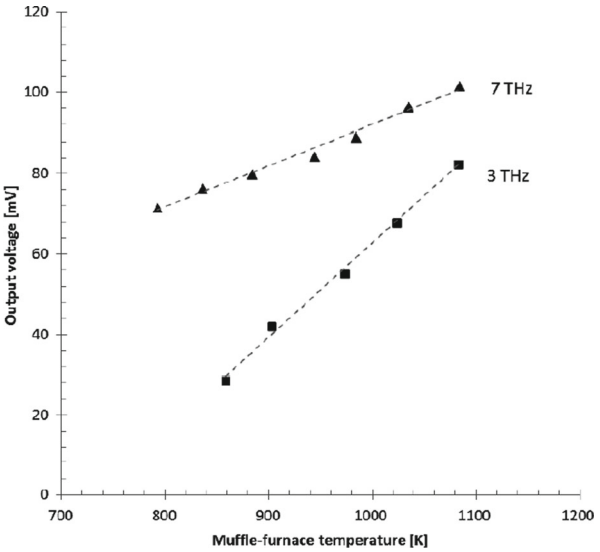

Fig. 9 The characteristic input temperature vs output voltage calibration of the 3 and 7 THz SOLAR-T

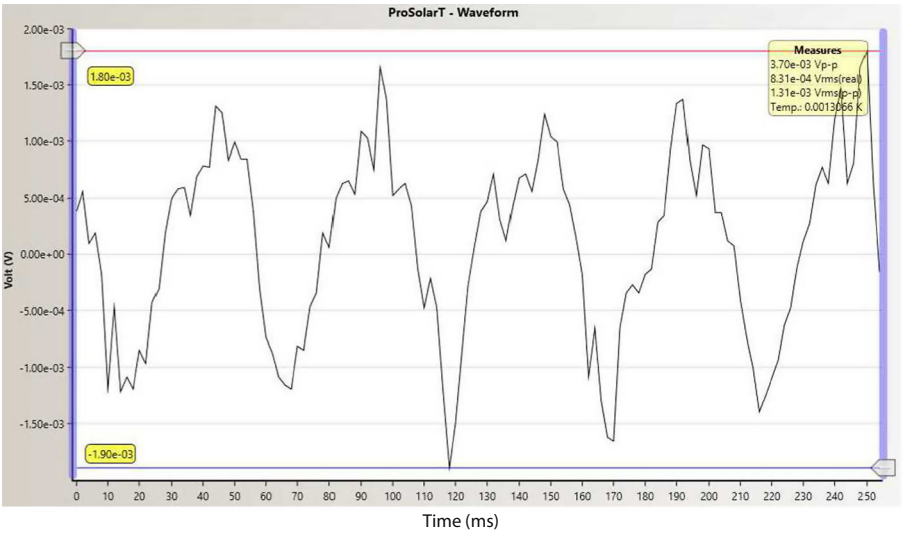

(a)

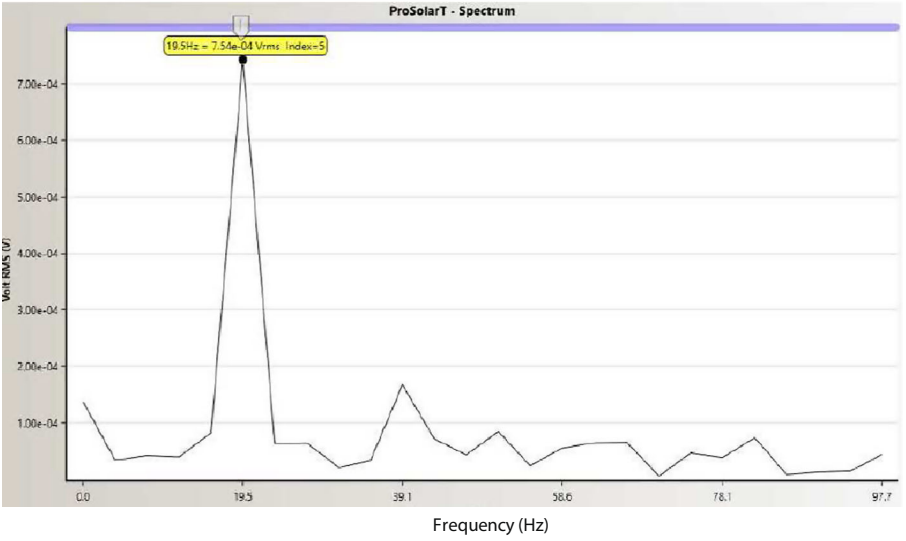

(b)

Fig. 10 Example for the 3 THz SOLAR-T ProSolarT data display of a sequence of six waveforms in (**a**) as response to the chopper to an arbitrary input heat source. **b** The Fourier transform for 128 points read at a rate of 500 Hz, producing the data points for the time series exhibited in Fig. 11

provide the reading at that time. Figure 11a and b shows the output time profile for 30 min of measurements at 3 and 7 THz respectively, with about 7100 data points smoothed with 11 points (corresponding to 2.8 s). The peak-to-peak fluctuations are

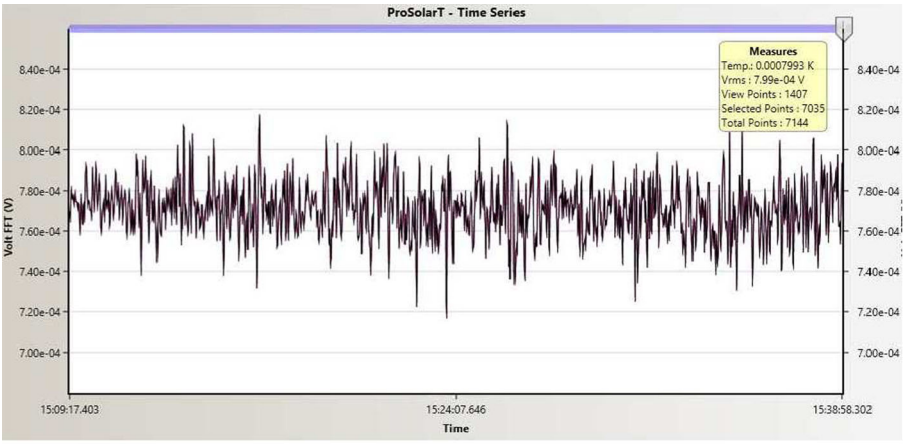

(a)

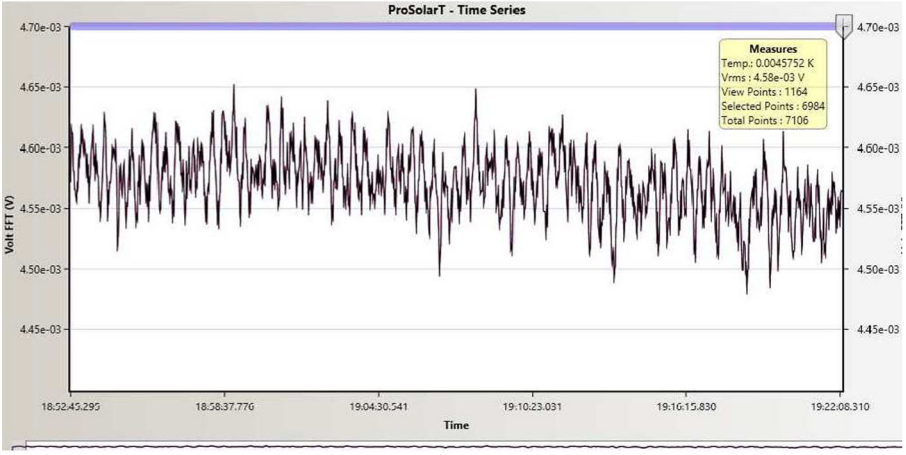

(b)

Fig. 11 Examples of nearly 30 min of data acquired with time resolution of 256 ms, smoothed with 11 points (i.e. 2.8 s). **a** at 3 THz, and **b** at 7 THz. The peak-to-peak voltage variations correspond to about 0.5 K using the temperature/voltage calibration shown in Fig. 9

of about 5 10^{-2} mV at 3 THz and of 7 10^{-2} mV at 7 THz. From the calibration curves shown in Fig. 9 we obtain peak-to-peak fluctuations of the order of 0.2 K at 3 THz and of 0.7 K at 7 THz which corresponds to small solar burst flux density, as it will be shown later.

The SOLAR-T photometers minimum detectable flux densities ΔS can be estimated. The Rayleigh-Jeans approximation for blackbody emission remains valid in the THz range [26]. The burst flux density is related to the excess temperature variations ΔT, above the observed baseline, according to the well known relationship [23] $\Delta S = 2\ k\ \Delta\ T/A_e$ where k is the Boltzmann constant and A_e the effective aperture

area, $A_e = \eta_a A_p$ where η_a is the aperture efficiency and A_p the aperture physical area.

The aperture efficiency is estimated as the product of several transmissions: the TydexBlack membrane, TPX and metal mesh band-pass filters in front of the Golay cell, the input TPX window, the physical blockage of subreflector holding structure, and rough reflector transmission. At laboratory conditions the air transmission must be added.

4.3 Telemetry performance

To monitor the THz photometers principal data acquired on board, clock, and auxiliary measurements are transmitted to ground by telemetry using the Iridium satellite network. The telemetry module TM module is housed in an aluminum milled box sized 15 cm × 7 cm × 5 cm, coupled to the SOLAR-T main case (Fig. 6c), except for the antenna which is assembled in adequate position in the balloon boom. The balloon-to-ground transmission latency, still being verified through more extensive tests, is approximately 20 s.

The completed SOLAR-T 3 and 7 THz photometer system coupled to data acquisition and telemetry modules have been assembled for the definitive performance tests, as illustrated in Fig. 12. The SOLAR-T Iridium antenna requires a wide angular field of view. We have placed it at the top of a mast (instead of lifting up the entire payload). One uncalibrated high temperature source has been placed in front of each photometer. Sets of 20 min of data acquired, with 0.256 ms resolution, were stored "on-board" the SOLAR-T, transmitted to the Iridium satellites, and received back by the ground station. Several tests were done with the transmitted data received back without any losses.

A separated identical data acquisition, storage and Iridium transmission and reception system was also built in the respective modules for redundancy purposes [15, 24].

5 Laboratory solar disk scan measurements

5.1 The "artificial Sun" setup

To evaluate the SOLAR-T THz photometers actual response to solar observations in laboratory, simulating realistic conditions in outer space, an artificial Sun setup was constructed, to be scanned across by the 3 and 7 THz photometers. The design schematics arrangement is shown in Fig. 13. The testing assembly is shown in Fig. 14. A hot blackbody source placed at the focus of a concave mirror radiates through a diaphragm, producing an angular size similar to the Sun in the sky after reflection by the concave mirror. Parallel rays reflected by the concave mirror are again reflected by a flat mirror and directed into the SOLAR-T telescopes. The artificial solar disk scans are obtained by displacing the hot source behind the diaphragm. The angular scan displacements are $\tan^{-1}(\delta\, 1/F)$, where $\delta 1$ is the hot source displacement, and F the concave reflector focal length.

Fig. 12 Realistic operational tests performed with SOLAR-T "on-board" setup, with hot source in front of telescopes, coupled to Iridium antenna at the top of the mast. Results are shown in Fig. 13

The "artificial" Sun setup and SOLAR-T were installed at Propertech laboratory to perform drift scans experiments, to simulate actual observations and respective calibration.

5.2 Drift scans of the "artificial" Sun source

The artificial Sun blackbody temperature was set at 743 K. The "artificial" disk flux density can be calculated using the well known formula [23] $S = 2\ k\ T\Omega/\lambda^2$ where k is the Boltzmann constant, T the disk temperature, Ω the solid angle for the apparent artificial solar disk diameter of $0.43°(5.1510^{-5}$ sr) and λ the wavelength. We calculate the full disk flux densities corresponding to a 743 K blackbody:

$$\begin{aligned} S &= 0.810^{-16}\ \mathrm{Wm^{-2}\ Hz^{-1}}\ \text{at 3 THz} \\ S &= 610^{-16}\ \mathrm{Wm^{-2}\ Hz^{-1}}\ \text{at 7 THz} \end{aligned} \quad (1)$$

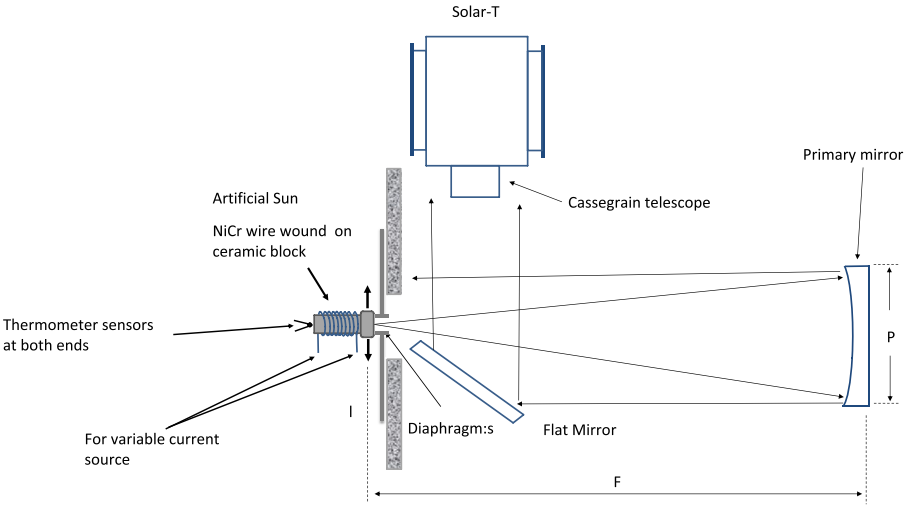

Fig. 13 The design of the "artificial Sun" arrangement to simulate scans of disk radiation in front of the THz photometers. The hot source at left is at the focus of a concave reflector (diameter P = 200 mm) to produce parallel rays, which are reflected by a flat mirror at 45° into the THz photometer, one each time. The main design parameters are F = 600 mm, diaphragm size s = 4.5 mm, SOLAR-T 76 mm with Cassegrain focal length of f = 580 mm. The diaphragm angular size as seen from the SOLAR-T telescopes is $\tan^{-1}(s/f) = 0.43°$, slightly smaller than the actual Sun diameter. The blurred "artificial" solar disk image size at the input of the Golay cell becomes $d = 580 \times \tan 0.43° = 4.3$ mm, smaller than 10 mm photon trap cone at the input of the Golay cell sensitive detection membrane

The predicted power at the Golay cell inputs can be expressed by ($S\ A_e\ \Delta f$), where A_e is the effective aperture and Δf the band-pass at each frequency. $A_e = \eta_a\ A_p$,

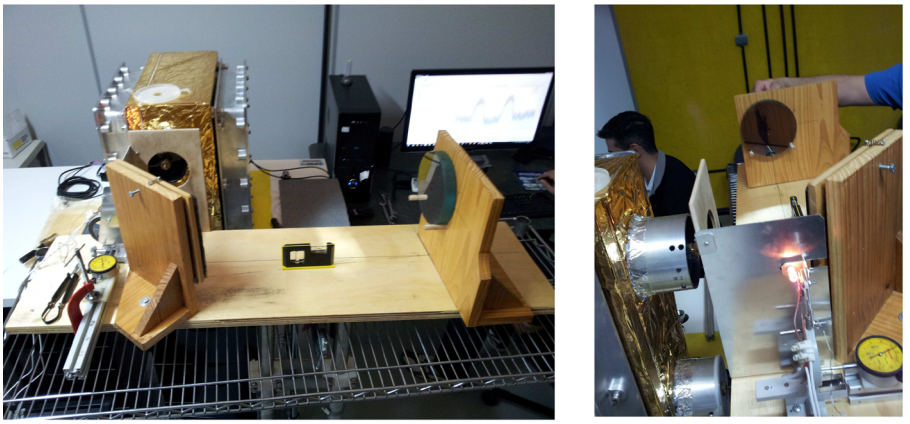

(a) **(b)**

Fig. 14 The "artificial" Sun setup installed in front of one of the SOLAT-T telescopes for practical disk scans measurements. **a** front view of the setup, with SOLAR-T telescopes in the background. **b** the heated blackbody and scanning mechanism, with the SOLAR-T telescope being tested at left

where $A_p = 4.5\ 10^{-3}$ m^2 is the primary reflector physical area and η_a the product of all transmission factors:

- the measured effect of the primary Cassegrain reflector roughness (0.9);
- aperture physical blockage (0.85);
- transmission of TPX window between the case and the telescope (0.8 at 3 THz; 0.6 at 7 THz) [25];
- transmission of sandwich TPX + BlackTydex membrane + metal mesh band-pass filter (0.35 at 3 THz and 0.29 at 7 THz, see Fig. 5);
- air transmission at laboratory setup of approximately 1 dB/m at both 3 and 7 THz [27]. For path of about 1.2 m we get 0.75.
- the transmission at two reflections on the aluminum coated concave and flat mirrors are nearly 1 for both frequencies (http://www.molalla.com/members/leeper/refcoat.pdf (2014)).

We obtain $\eta_a \sim 0.16$ at 3 THz and $\eta_a \sim 0.1$ at 7 THz, with $A_e \sim 7\ 10^{-4}$ m^2 and $4.5\ 10^{-4}$ m^2 at 3 and 7 THz, respectively. The half-power band-pass is about 0.4 THz at 3 THz and of 1.2 THz at 7 THz [22]. Therefore, the predicted power at the Golay cell inputs is about

$$\begin{aligned} P &= 1.7\ 10^{-7}\ \text{W at 3 THz} \\ P &= 4.3\ 10^{-8}\ \text{W at 7 THz.} \end{aligned} \tag{2}$$

In Fig. 15 we show examples of the "artificial" solar disk drift scans obtained in these conditions. For comparison, refer to the plot given in Fig. 2. Data has been smoothed on 50 points which net effect was to reduce ripple fluctuations to less than 10 μV over 35 arc-seconds. The upper panel shows the 3 THz drift scan with nearly 90 arcmin half power width. It corresponds to the artificial solar disk 4.3 mm image transit over the 10 mm cone extension. The second panel from top shown the derivative, which indicate an approximate average the disk half angular size of 35 arcmin. The solar image transit between the two inner half-power intensities, of roughly 50 arcmin, corresponds to the telescope acceptance angle, through which the whole solar disk image remains on the detection cone opening. The two lower panels are for a scan on the 7 THz photometer. The measurements are basically the same. These results are consistent with the concentrator principle described in Section 2.

The solar disk amplitudes in excess to the pre existing level are approximately of 0.7 mV at 3 THz and 7 mV at 7 THz. From the characteristic photometers' calibration curves, Fig. 9, (i.e. 4.2 K/mV at 3 THz and 9.8 K/mV at 7 THz) the maximum scan intensities correspond to excess input temperatures of 3 K and 69 K at 3 and 7 THz respectively. Since the pre-existing level corresponds to the ambient temperature (at about 300 K), the observed artificial solar disk temperatures becomes $\Delta T = 303$ K at 3 THz and 369 K at 7 THz. The observed input power $P = 2\ k\ \Delta T\ \Delta f$. We obtain

$$\begin{aligned} P &= 3.4\ 10^{-9}\ \text{W at 3 THz} \\ P &= 10^{-8}\ \text{W at 7 THz} \end{aligned} \tag{3}$$

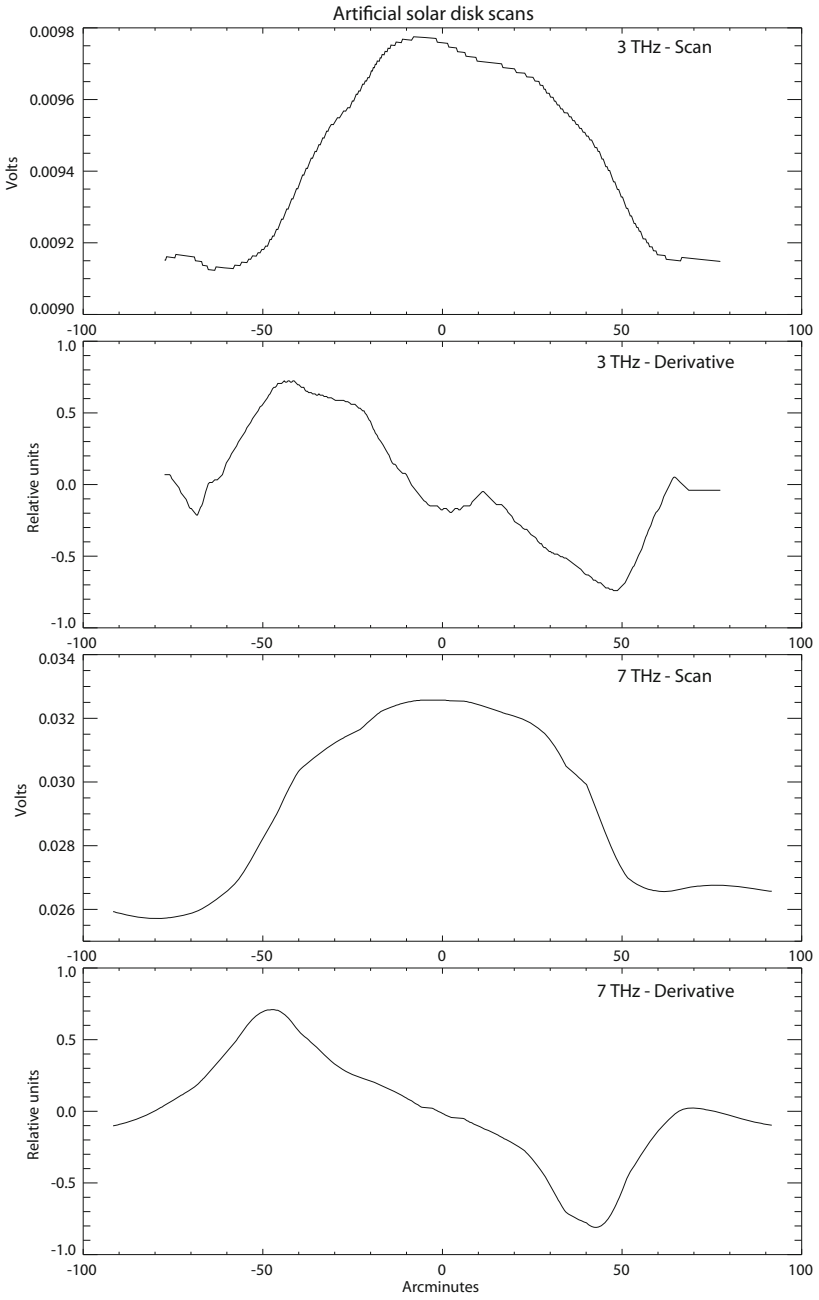

Fig. 15 "Artificial" solar disk drift scans SOLAR-T responses, for a disk temperature of 743 K, displayed in output mV vs angular displacement. 256 ms data readings were smoothed for 50 points. Plots for the 3 THz photometer at the top, with derivative in the second panel from the top; for the 7 THz photometer in the third panel from the top and corresponding derivative at the bottom

Which converted into observed disc flux densities $S = P/(A_e \Delta f)$:

$$\begin{aligned} S &= 1.2\ 10^{-17}\ \mathrm{W\ m^{-2}\ Hz^{-1}} \text{ at 3 THz} \\ S &= 2\ 10^{-17}\ \mathrm{W\ m^{-2}\ Hz^{-1}} \text{ at 7 THz} \end{aligned} \quad (4)$$

that compares within less than an order of magnitude at 3 THz, and of about one order of magnitude at 7 THz, to the calculated values shown before, despite the assumptions adopted and the uncertainties of the laboratory measurements.

The sensitivity to detect THz flares excess temperatures, and corresponding fluxes, depend on the data smoothing. As shown before, for 10 data points smoothing, SOLAR-T can detect ΔT less than 0.5 K at sub-second time resolution. Outside the atmosphere, the air transmission factor is neglected, and the aperture efficiencies improved to $\eta_a = 0.2$ and 0.15 at 3 and 7 THz, respectively. The r.m.s. flux densities calculated from $\Delta S \sim 2\ k\ \Delta T/A_e$, for $\Delta T \approx 0.2$ K at 3 THz and 0.7 K at 7 THz, becomes less than about 80-400 SFU at 3 and 7 THz respectively. For larger smoothing, the sensitivity improves substantially.

6 Final remarks

We have shown the performance of the 3 and 7 THz photometers using Golay cell detectors, low pass and band-pass filters, integrated to data acquisition, processing, and telemetry. The output voltage level is very stable, which is a necessary condition to detect small relative changes. The total voltage output is proportional to the temperature of the source placed in front of the telescopes. The output noise fluctuations proportionality to the input temperature fluctuations remain the same for different input heat source areas. The relative excess fluctuations are irrespective from the baseline level of the time series. Relative one r.m.s. changes observed $\Delta V \propto \Delta T$ correspond to excess transient solar burst fluxes of the order of 80-400 SFU, at subsecond time resolution.

The laboratory tests have shown that the performance of the THz photometers is consistent with the design concept. The artificial solar disc image size (of about 4.3 mm) is smaller than the Golay cell input cone (10 mm), producing an acceptance angle of about 50 arcmin. Therefore the requirement for pointing and tracking accuracy is of about 20 arcmin (i.e., the 50 arcmin—30 arcmin solar disc apparent diameter).

In outer space SOLAR-T observations shall refer to scans of brighter disks, of about 4500 K (±500 K) [28], i.e. flux densities of $4.8\ 10^{-16}$ W m^{-2} Hz^{-1} at 3 THz and $3.6\ 10^{-15}$ W m^{-2} Hz^{-1} at 7 THz. Similarly the observed solar scans will be measured above the photometers ambient input TPX windows temperature (see Fig. 2). In practice, the solar scans will provide the flux density scale calibration for flares, as done by usual full Sun patrol radio telescopes.

The SOLAR-T experiment shall fly on two long duration stratospheric balloon missions (2014–2016). One coupled to the gamma ray experiment GRIPS [25] of University of California, Berkeley, USA, over Antarctica (two weeks), and another over Russia (7–10 days) in cooperation with the Lebedev Physical Institute, Moscow,

Russia, on an autonomous automatic Sun tracking gondola under development. Solar flare observations at 3 and 7 THz by SOLAR-T shall provide the spectral indices trends, which may be positive, negative or flat, depending on the emission mechanisms involved. SOLAR-T observations may be complemented by ground-based observations carried out at El Leoncito, Argentina Andes, at 45, 90, 212 and 405 GHz when occurring in the same common observing hours (in the time interval of 11–21 UT), allowing the derivation of the complete burst spectral shape description, needed for further tests of different interpretation models.

Acknowledgments The authors acknowledge discussions and advices received from various experts in the areas of nanotechnology, materials, sensors, data acquisition along the developments which led to the construction of SOLAR-T, specially to J,A. Diniz, E. Grossman, G. Hurford, M.K. Lebedev, R. Lin, A. Semery, A. Shih, J. Swart, G. Trottet and M.B. Zakia. The authors thank one anonymous referee which careful corrections and useful suggestions have improved this presentation. This program was partially funded by Brazil agencies FAPESP (Proc.2010/51861-8), CNPq INCT-NAMITEC, CNPq, and Mackpesquisa, Argentina CONICET and US AFOSR.

References

1. Kaufmann, P., et al.: A new solar burst spectral component emitting only in the terahertz range. Astrophys. J. **603**, L121 (2004)
2. Silva, A.V.R., et al.: Evidence that synchrotron emission from nonthermal electrons produces the increasing submillimeter spectral component in solar flares. Solar Phys. **245**, 311 (2007)
3. Kaufmann, P., et al.: A bright impulsive solar burst detected at 30 THz. Astrophys. J. **768**, 134 (2013)
4. Fleishman, G.D., Kontar, E.: Sub-THz radiation mechanisms in solar flares. Astrophys. J. **709**, L127 (2010)
5. Krucker, S., et al.: Solar flares at submillimeter wavelength. Astronon. Astrophys. Rev. **21**, article id. #58 (2013)
6. Erickson, E.F.: SOFIA: the next generation airborne observatory. Space Sci. Rev. **84**, 91–100 (1985)
7. Poglitsch, A., et al.: The photodetector array camera and spectrometer (PACS) on the Herschel space observatory. Astron. Astrophys. **518**(L2), 1–12 (2010)
8. Degiacomi, C.G., Kneubühl, F.K., Huguenin, D.: Far-infrared solar imaging from a balloon-borne platform. Astrophys. J. **298**, 918–933 (1985)
9. Deming, D., Kostiuk, T., Glenar, D.: The Solar Infrared Explorer (SIRE): a small Explorer mission for solar physics. BAAS **23**, 1038 (1991)
10. Trottet, G., Klein, L., Molodij, G., Semery, A.: Far infrered observations of solar flares during the next solar maximum. In: 36th COSPAR Scientific Assembly, 13–23 July. Beijing, China, Abstract #1788 (2006)
11. Lawrence, J.S.: Infrared and submillimeter atmospheric characteristics of high Antarctic plateau sites. Publ. Astron. Soc. Pac. **116**, 482–492 (2004)
12. Suen, J., Fang, M., Lubin, P.: Global distribution of water vapor and cloud cover—sites for high-performance THz applications. IEEE Trans. THz Sci. Technol. **4**, 86–100 (2014). doi:10.1109/TTHZ.2013.2294018
13. Marcon, R., Kaufmann, P.: Método para maximizar ganho na detecção simultânea de radiação de fontes pequenas em campo extenso de visão. Brazil Patent Application, Universidade Estadual de Campinas and Instituto Presbiteriano Mackenzie, Patent filed March 30 (2011)
14. Marcon, R., et al.: Terahertz photometer to observe solar flares in continuum. J. Infrared Millim. Terahertz Waves **33**, 192–205 (2012)
15. Kaufmann, P., et al.: SOLAR-T: terahertz photometers to observe solar flare emission on stratospheric balloon flights. Proc. SPIE **8442L**, 1–9 (2012)
16. Fernandes, L.O.T., et al.: Photometry of THz radiation using golay cell detector. In: Proceedings of XXX URSI GA, Paper JP2.10, Istanbul (2011)

17. Marun, A.: Fotometría de banda ancha em la región terahertz (THz) del espectro electromagnético. MS thesis, Facultad de Ingenieria, Universidad de Buenos Aires, Argentina, April 17 (/2012)
18. Golay, M.J.E.: The theoretical and practical sensitivity of the pneumatic infra-red detector. Rev. Sci. Instrum. **20**, 816 (1949)
19. Kostiuk, T., Deming, D.: A solar infrared photometer for space flight application. Infrared Phys. **32**, 225 (1991)
20. Kornberg, M.A., et al.: Rough mirrors for the THz frequency range. In: Proceedings of the MOMAG 2008—13th SBMO and 8th CBMAG, Florianopolis, 7–10 September, 367 (2008)
21. Melo A.M., et al.: Metal mesh resonant filters for terahertz frequencies. Appl. Opt. **47**, 6064 (2008)
22. Bortolucci, E.C., et al.: THz band-pass resonantmetal mesh filters for a space solar photometry experiment. In: VII Workshop on Semiconductors and Micro & Nano Technology - Seminatec, 77 (2012)
23. Kraus, J.D.: Radio Astronomy, 2nd edn, Chapter 6. Cygnus-Quasar Books, Powell (1980)
24. Kaufmann, P., et al.: The performance of THz photometers for solar flare observations from space. In: Proc. IMOC/SBMO/IEEE-MTT Conference, Rio de Janeiro (2013)
25. Shih, A.Y., et al.: The Gamma-Ray Imager/Polarimeter for Solar Flares (GRIPS). In: American Geophysical Union, Fall Meeting, abstract SM11B-1602 (2008)
26. Phillips, T.G.: Techniques of submillimeter astronomy, in Millimetre and submillimetre astronomy. In: Wolstencroft, R.D., Burton, W.B. (eds.) Lectures at Summer School, Stirling, Scotland, June 21–27, 1987, pp. 1–25. Kluwer Academic Publishers, Dordrecht (1988)
27. Yasuko, K., Takamasa, S.: Atmospheric propagation model of terhertz-wave. J. Natl Inst. Inf. Commun. Technol. **55**, 73–77 (2008) in http://www.intechopen.com/download/get/type/pdfs/id/37524(2014)
28. Gezari, D.Y., Joyce, R.R., Simon, M.: Measurement of the solar brightness at 345μ, 450μ and 1000μ. Astron. Astrophys. **26**, 409–411 (1973)